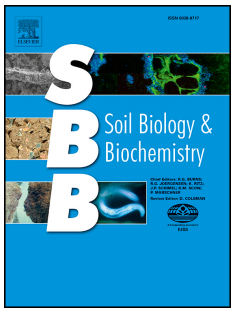

Automated sensor-based quantification of soil water retention and microbial respiration across drying conditions

Huijie Gan, Wayne Roper, Peter M. Groffman, Tom Morris, Karl Guillard

PII: S0038-0717(23)00049-4

DOI: https://doi.org/10.1016/j.soilbio.2023.108987

Reference: SBB 108987

To appear in: *Soil Biology and Biochemistry*

Received Date: 20 November 2022

Revised Date: 30 January 2023

Accepted Date: 18 February 2023

Please cite this article as: Gan, H., Roper, W., Groffman, P.M., Morris, T., Guillard, K., Automated sensor-based quantification of soil water retention and microbial respiration across drying conditions, *Soil Biology and Biochemistry* (2023), doi: https://doi.org/10.1016/j.soilbio.2023.108987.

Automated Sensor-Based Quantification of Soil Water Retention and Microbial Respiration Across Drying Conditions

Huijie Gan[1*], Wayne Roper[1], Peter M. Groffman[2,3], Tom Morris[1], and Karl Guillard[1]

[1]Department of Plant Science and Landscape Architecture, University of Connecticut, Storrs, CT

[2]City University of New York, Advanced Science Research Center at the Graduate Center, New York, NY

[3]Brooklyn College Department of Earth and Environmental Sciences, Brooklyn, NY

* Corresponding author:

huijie.gan@uconn.edu

University of Connecticut, 1376 Storrs Road, Storrs, CT 06269

Abbreviations: SOM: Soil Organic Matter; SWC: Soil Water Content; WHC: Water Holding Capacity;

Abstract

Understanding soil responses to climate-induced precipitation variability is important for improving global carbon models and the development of climate-resilient agriculture. However, our knowledge remains limited regarding factors that influence soil water dynamics and microbial respiration across drying conditions, partially hindered by the lack of easily accessible methodologies. We developed a low-cost, automated, and integrated system to simultaneously quantify microbial respiration and soil water retention in response to drought conditions. This system integrates a CO_2 sensor and a digital scale, enabling continuous measurement of CO_2 concentration and soil water loss by evaporation when soils are incubated with desiccants inside air-tight chambers. Here we show that the sensor platform provides accurate and repeatable CO_2 measurements when compared to a spectroscopy gas analyzer and the alkali trap method. Using the sensor platform, we further demonstrated that averaged microbial respiration of rewetted soil over 4-day incubation declined as management intensity increased following the order of Till ≤ NoTill ≤ Till_fallow ≤ NoTill_fallow = Hay field < Forest. These soils were air-dried for two years before use in incubation experiments, and microbial respiration upon rewetting showed a unimodal response, which rapidly increased and peaked within 12 hours except for in forest soils that exhibited a delayed response with respiration peaking at 30 hours. Under drying conditions, rewetted soil from the Hay field showed lower water loss than other soils. Volumetric water content at the end of the drying period increased in the order of Till ≤ NoTill < Till_fallow ≤ NoTill_fallow = Hay field< Forest. We posit that this sensor platform provides a powerful tool for functional soil health assessments and fundamental understanding of soil water dynamics and microbial activities in responses to climate-induced water stress.

Keywords: CO_2 sensor; Drought resistance; Microbial respiration; Soil health; Soil water evaporation

1. Introduction

The frequency of severe floods and prolonged droughts is predicted to increase in many regions of the world due to intensified hydrological cycles associated with global warming (Dai, 2013). The ability of soil to buffer extreme weather events is critical in mitigating impacts of climate change on crop production. A soil that absorbs more water from rains without ponding or runoff and has slower evaporation afterward would particularly be desirable for climate-resilient agriculture (Baveye et al., 2020). Common measurements of soil hydraulic properties, such as water holding capacity, hydraulic conductivity, and water retention curves, provide important insights in predicting soil-water dynamics in response to variable precipitation (Seneviratne et al., 2010). However, obtaining data on these properties normally requires significant investments in time and labor and/or expensive analytical equipment. An inexpensive and rapid method for measuring soil water retention under drying conditions could facilitate the evaluation and prediction of soil responses to climate-induced precipitation variability.

Changes in soil water content (SWC) following precipitation have significant influences on soil microbial processes and soil organic matter (SOM) dynamics. The release of CO_2 and other greenhouse gases during wet-dry cycles is highly variable over time and difficult to predict (Borken and Matzner, 2009). Empirical studies often rely on discrete temporal measurements, which are likely to miss "hot moments" of gas flux from soils (van Groenigen et al., 2015). A flush in microbial activity is often observed upon rewetting dry soil, however, many unknowns remain regarding the underlying physiochemical and biological mechanisms of this flush (Schimel, 2018). Obtaining high-quality empirical data for an accurate representation of soil microbial responses to soil water variability is critical for improving biogeochemical models of greenhouse gas emissions and soil organic carbon (SOC) dynamics (Moyano et al., 2013).

The flush of CO_2 from short-term incubation of rewetted soils is also widely used as an indicator of soil quality or soil biological health (Franzluebbers, 2018; Wander et al., 2019). This indicator is referred to as short-term soil respiration, CO_2 burst, soil test biological activity, or C mineralization potential (Norris et al., 2020), and has been found to be responsive to soil management practices and to be associated with other soil properties such as soil microbial biomass, labile C pool, and N mineralization potential (Franzluebbers et al., 2000). Conventional methodologies for soil respiration measurements include the alkali trap method and the use of

gas analyzers to quantify CO_2 accumulation from microbial respiration (Parkin et al., 1997). These methods require substantial labor/time input and often only provide a few discrete measurements during soil incubation. The use of hazardous chemicals or specialized instruments has largely restricted such analyses to commercial soil testing labs or service-providing universities, which makes routine soil respiration measurements cost prohibitive. There have been attempts to make less expensive options using commercial CO_2 sensors (Joshi Gyawali et al., 2019), but the adoption of these approaches has been hindered by the complex engineering experience required to assemble and use sensors.

The main objectives of our study were to: (1) develop a user-friendly sensor platform to provide continuous and simultaneous measurements of SWC and microbial respiration under drying conditions in a laboratory environment; (2) evaluate the reliability of this platform as compared with a spectroscopy gas analyzer and the alkali trap method; and (3) compare measurement results from soils with different land use and management histories to assess the usefulness of the sensor platform in soil health assessments. We expect that soils under low management intensity would have higher water retention and microbial respiration compared to intensively managed soils across drying conditions.

2. Materials and Methods

2.1. Construction of the sensor platform

2.1.1. Design overview

The platform consists of an air-tight chamber equipped with multiple sensors: a CO_2 sensor to measure CO_2 accumulation from microbial respiration, a digital scale to quantify changes in SWC during soil incubation, a temperature sensor, and a humidity sensor to track changes in temperature and humidity inside the chamber (Fig. 1). A desiccant is placed inside the chamber to prevent excessive humidity. The sensors and digital scale are controlled by a microcontroller equipped with a real-time clock and a data logger for automatic data storage as well as a display screen for real-time monitoring of results. All electronics are commercially available, cost less than USD $150 (at the time of data collection), and can be assembled with little engineering experience.

The platform follows the principle of a modular design, allowing modification and independence of individual functional components. For example, the CO_2 sensor component can

be used in other containers (e.g., Mason jars) commonly used for soil incubation studies (Fig. S3a) or adapted for use in the field independent of the digital scale. Similarly, the digital scale can be used without desiccants in an open-air environment to monitor soil water evaporation under natural air-drying conditions.

2.1.2. Hardware

The measurement system includes four environment sensors (a CO_2 sensor, a load cell with a signal converter, a temperature sensor, and a humidity sensor), a microcontroller, a data logger, and a display screen. These components can be obtained from various suppliers with different technical specifications and market prices. The CO_2 sensor we used is a nondispersive infrared (NDIR) sensor with a stated accuracy of ± 30 μmol^{-1} mol^{-1} (referred to ppm afterward) from 400–10,000 ppm (SCD-30, Adafruit Industries, New York, NY, USA). Such CO_2 sensors are highly sensitive and can respond to changes in CO_2 concentration within seconds. This CO_2 sensor includes temperature (accuracy: ± 0.4 ºC at 25 ºC) and relative humidity sensors (accuracy: ± 3%). The load cell was obtained from a common household scale (500g Digital Kitchen Scale US-KA8B, AMIR) and then connected to an analog-to-digital converter (NAU7802 Qwiic Scale, SparkFun Electronics, Boulder, CO, USA). Many microcontrollers can be used to configure and control these sensors; we used an ESP32-based board (HUZZAH32 Feather Board, Adafruit Industries, New York, NY, USA) because of its ease in incorporating data-loggers and display screens. These electronics can be powered by portable batteries (9 V-12 V) or common USB ports. The environmental sensors were stationed inside an air-tight chamber (25 cm × 18 cm × 15 cm, LocknLock Inc., South Korea), with wire connections to the microcontroller and other electronics secured outside of the chamber.

2.1.3. Software and sensor calibration

The programing languages to control the electronics are compiled through the open-source Arduino Software (https://www.arduino.cc/en/software), a widely used integrated development environment (IDE) for writing and uploading code to circuit boards. Commercially available sensors usually contain detailed instructions on how to configure sensors and example codes on Arduino IDE for data acquisition. Example codes for sensor communication and data acquisition used in this study is available on Adafruit learning guides (https://learn.adafruit.com/adafruit-scd30/arduino).

Load cells for the digital scales were calibrated using a two-point calibration (zero weight, and a standard 50 g weight) assuming a liner response. The CO_2 sensors were calibrated to 400 ppm when exposed to fresh outdoor air. For this study, we configured the sensors to record CO_2 concentration every minute.

2.2. Testing of sensor accuracy, noise, and signal drift

CO_2 sensors were validated by comparing their readings with readings from a spectroscopy gas analyzer with high precision (± 5 ppb CO_2, Picarro G2301, Picarro Inc., Santa Clara, CA, USA). CO_2 sensors with portable batteries and other associated electronics were placed in a Mason jar (8-cm in diameter × 18 cm in height, Ball Corporation, Broomfield, Colorado, USA). The lid of the jar had two customized tubing fittings, which were connected to the Picarro gas analyzer and an air pump to allow air inside the jar to circulate through the gas analyzer in a closed loop (Fig. 2b). Five measurement runs were conducted with a gradient of CO_2 concentrations ranging from ambient to over 8000 ppm. Elevated CO_2 concentrations were created by breathing into the Mason jar right before closing the lids. For each run, readings from CO_2 sensors and the Picarro gas analyzer were recorded every 5 minutes for 15 minutes.

To evaluate the noise level and potential signal drift of the CO_2 sensors over time, a gradient of CO_2 concentrations (~500 ppm to ~6000 ppm) was created inside incubation chambers. Similarly, a series of standard weights (0 g, 10 g, 30 g, 50 g, 70 g, and 100 g) were placed on the load cells to test accuracy and precision of the digital scales. High CO_2 concentrations were created by breathing into chambers before closing lids, which were further sealed with duct tape to minimize air leakage. The sensor chambers were then placed inside an incubator at 28.5 °C (Model 1535 Incubator, VWR Scientific Inc., Pennsylvania, USA). Sensors and other electronics were powered through USB ports inside the incubator and sensor readings were recorded every minute for 48 hours.

2.3. Experiment I: Comparing sensor-based microbial respiration with the conventional alkali trap method

2.3.1. Soil collection

Soils were collected from June to July 2020 from six field sites under diverse land use and management practices: silage corn (*Zea mays* L.) fields with conventional tillage (Till) for more than 50 years or no-till practice (NoTill) for more than 10 years, research plots with a history of

more than 40 years of conventional tillage (Till_fallow) or no-till practices (NoTill_fallow) before being fallow for 5 years, a grassy field managed for hay production for more than 100 years (Hay), and a mixed deciduous forest that has been developing on abandoned cropland for more than 150 years (Forest). Within each field, three soil pits sized 1-m deep and 1-m wide were excavated for pedon description. Surface soils (0–5 cm) were collected from each pedon. There were two pedons within the hay fields, resulting in a total of 17 soils for use in this study. Field-moist soils were sieved to < 8 mm and then air-dried and stored in plastic bags for two years before use in the rewetting experiments. All soils have a sandy loam texture, but soil total C content increases as management decreases following the order of Till = NoTill=Till_fallow < NoTill_fallow=Hay<Forest (Table 1).

2.3.2. Microbial respiration of rewetted soils in 4-day incubations

To evaluate the reliability of the CO_2 sensor in measuring microbial respiration compared to the conventional alkali trap method, we incubated soils inside sensor chambers following a procedure commonly described as short-term C mineralization or CO_2 flush of re-wetted soils (Franzluebbers, 2018). Briefly, 20 g of air-dry soils were re-wetted with 7.5 mL of water inside a 150-mL plastic container (5.8-cm diameter × 7.2-cm height). The re-wetted soil was then placed inside the sensor chamber (regular, 4500 mL in volume, Fig 1), which was incubated at 25 °C in a controlled environment incubator (Intellus Environmental Controller, Percival Inc., Iowa, USA). Readings for CO_2 concentrations, temperature, and relative humidity inside the chamber were recorded every minute for 4 days. To evaluate whether the chamber volume would affect sensor detection of CO_2 emission, we tested a subset of soils (two NoTill soils and two Forest soils) placed inside Mason jars of different sizes (473 mL, and 1890 mL) that are commonly used for soil incubation (Fig. S3).

For the alkali trap method, re-wetted soils with the same soil water ratio (20 g air-dry soil: 7.5 mL water) were placed inside Mason jars (8-cm diameter × 12-cm height) following the procedure described in the Cornell Comprehensive Assessments of Soil Health Manual (Schindelbeck et al., 2016). A 10-mL glass beaker consisting of 9 mL of 0.5 M KOH was placed on a stand over the soil surface to serve as an alkali trap. The jars were sealed with the two-part lids and then placed in the same incubator used for the sensor study at 25 °C. Electrical conductivity (EC) of the KOH trap solution was measured before and after a 4-day incubation

using a benchtop EC meter (Orion Versa Star Pro, Thermo Scientific, Waltham, MA, USA). Total amount of CO_2 respired was calculated based on changes in EC in the alkali trap relative to EC in pure KOH and saturated K_2CO_3 solution (Schindelbeck et al., 2016). Averaged microbial respiration rate (μg CO_2-C g^{-1} soil hr^{-1}) over the 4-day incubation was calculated for comparisons with the sensor method.

2.4. Experiment II: Soil water dynamics and microbial respiration under drying conditions in 7-day incubations

To simulate a wet-dry cycle, soils were rewetted until field capacity and then incubated together with desiccant inside the sensor chambers. Soil columns were created by packing air-dried soil into 50-mL conical plastic tubes (3-cm diameter × 11-cm height, Corning Inc., NY, USA). The top half of the plastic tube was cut off to allow faster dispersion of water vapor, and a small hole (~2 mm in diameter) was drilled in the bottom of the tube to allow water drainage. A piece of filter paper (Whatman no. 42, Cytiva Life Science, MA. USA) was placed inside the tube, and wetted with deionized water. The weight (W_{tube}) of the tube with wet filter paper was recorded.

A total of 22.5 mL of soil (5 cm in height) was loosely packed in the tubes by gently tapping the side of the tubes while adding soil. Differences in bulk density among the repacked soils (Table 1) resulted in net dry soil weight (W_{soil_dry}) ranging from 14.9 g (Forest soil) to 29.7 g (Till soil). For each soil column, 25 mL of water was added to the top, simulating a 3.5 cm precipitation event. The re-wetted soil columns were allowed to drain for about one hour until water stopped dripping from the bottom, which was considered to be field capacity SWC. The soil columns were then placed on the digital scale inside the chambers with the total initial weight (W_{T0}) recorded, and SWC at field capacity was then calculated as the difference between W_{T0} and (W_{tube} + W_{soil_dry}). Inside each sensor chamber, 35 g of anhydrous $CaCl_2$ (Fisher Chemical, Fisher Scientific, NH, USA) was spread out evenly in a petri dish (10-cm in diameter) to maintain a low relative humidity (15–30%) during the incubation. All sensor chambers were then placed inside an incubator at 28.5 °C to accelerate drying for seven days. All 17 soils from Experiment I were used for this experiment. To examine within-soil variability, a few soils from the NoTill_fallow, Till_fallow, and the Hay fields were replicated, which resulted in 21 independent incubations.

2.5. Experiment III: Comparing microbial respiration under consistent vs. drying moisture conditions in 7-day incubation

Six soil samples from NoTill_fallow and Till_fallow sites were incubated for approximately seven days at 28.5 °C under both consistent moisture conditions as described in Experiment I and drying conditions as described in Experiment II. To allow direct comparisons based on mass, all 12 incubations started with 20 g of dry soil. Gravimetric SWC was maintained at 3.75 $cm^3\ g^{-1}$ for soils under consistent moisture conditions. In comparison, SWC declined from 0.50 $cm^3\ g^{-1}$ to 0.10 $cm^3\ g^{-1}$ when incubated under drying conditions.

2.6. Data processing and statistics

Senor readings are stored in a micro-SD card in a text file, which can be easily exported into data analysis software. To reduce data noise, raw CO_2 and weight readings of every minute were first averaged by the hour before further analyses.

Cumulative CO_2 respired (ppm) at time *t* was calculated by subtracting initial CO_2 concentrations (t = 0) from CO_2 concentrations at time *t*. To further reduce sensor noise, hourly moving averages of CO_2 concentrations were calculated using a moving window of four hours; the hourly respiration rates (ppm per hour) were then calculated by taking the difference of CO_2 moving averages between consecutive hours. The moving window of four hours was chosen to minimize the effects of short-term fluctuation in sensor response (Fig. S2). To examine whether reducing the data to the hourly averages would affect the temporal respiration pattern, we also calculated respiration rates for a subset of soils using the raw data with the frequency of every minute. The respiration rate was further converted to the amount of CO_2-C per unit of soil per unit time ($\mu g\ CO_2\text{-}C\ g^{-1}$ soil hr^{-1}) based on the ideal gas law, the volume and the temperature of the incubation chamber, and the amount of soil used for each sample. Averaged respiration rates within each day or over the entire incubation period were calculated by averaging the hourly respiration rates within specific time windows.

Cumulative water evaporated at time *t* was calculated by subtracting weight at time *t* from the initial weight (W_{T0}), assuming 1 g of weight loss from the soil column equals to 1 mL of water evaporated. Relative water evaporation (%) was calculated by dividing cumulative water evaporation by initial SWC at field capacity. Volumetric SWC ($cm^3\ H_2O\ cm^{-3}$ soil) at time *t* was calculated by taking the difference between initial SWC and cumulative water evaporation

at time *t*. Gravimetric SWC (cm^3 H_2O g^{-1} soil) was also calculated based on volumetric SWC and the net dry soil weight of each soil column. To calculate evaporation rates, a moving average of weight data were first calculated using a moving window of four hours, and hourly evaporation rates (cm^3 H_2O cm^{-3} soil hr^{-1}) were calculated by taking the difference of moving averages between consecutive hours. Averaged evaporation rates within each day or over the entire incubation period were calculated by averaging the hourly evaporation rates within specific time windows.

For Experiment I, a linear model was conducted to compare microbial respiration between the sensor method and the alkali trap method, and Wald test was used to evaluate if the slope of the linear model deviated from 1 (Fox et al., 2007). A pairwise *t*-test was used to evaluate if the two methods provided similar measurements of microbial respiration. For Experiment I and II, a two-way (land use × day) ANOVA was used to evaluate how land management and time since rewetting affected respiration and evaporation rates. Pearson correlation coefficients were calculated to evaluate the relationships between soil C content, SWC, and microbial respiration. For Experiment III, a three-way ANOVA (land use × day × incubation method) was used to evaluate if microbial respiration differed between the two incubation conditions (rewetted and maintained at consistent moisture levels vs. rewetted to field capacity and continued drying). Due to the high number of soil groups to compare (treatment levels = 6) and the small sample size per group ($n = 3$), we used alpha = 0.10 to increase the power to detect differences among groups. When source effects were significant, treatment means were separated using *post hoc* pairwise comparisons with Tukey's HSD tests at $\alpha = 0.10$.

All data analyses and visualization were performed in R software version 2.15 (R Core Team, 2016) with the following packages: *zoo* for calculating the moving averages (Zeileis and Grothendieck, 2005), *ggplot2* for data visualization (Wickham, 2016), *mgcv* for fitting smooth lines for hourly respiration and evaporation data (Wood, 2017), *car* for the Wald test of the linear models for method comparisons (Fox et al., 2007), and *emmeans* for ANOVA and pairwise comparisons (Lenth and Lenth, 2018).

3. Results

3.1. Sensor accuracy, noise, and signal drift

The digital scales provided accurate readings of known standard weight ranging from 0 g to 100 g (Fig. S1). There was no apparent signal drift over 48 hours under consistent temperature, with a noise of approximately ± 0.3 g around expected values (Fig. S1). Consistent scale readings are critical to accurately track changes in soil weight induced by water evaporation as soil dries.

CO_2 readings from sensors were highly correlated with gas analyzer readings within the range of 500–8000 ppm (Fig. 2a, $r^2 = 1$, $p < 0.001$). The slope of the regression did not deviate from 1, although CO_2 sensors had consistently higher readings (+ 46 ppm) than the gas analyzer (paired *t*-test, $p = 0.03$). There was no apparent drift of CO_2 readings inside empty incubation chambers for concentrations ≤ 4900 ppm (Fig. S2). CO_2 readings of ambient indoor air averaged 522 ppm over 48 hours with a minimum of 491 ppm and a maximum of 542 ppm, consistent with the stated noise level of ± 30 ppm. However, incubation chambers with very high CO_2 concentrations (>4900 ppm) declined between 300–400 ppm after 48 hours, possibly because chambers were not completely air-tight (Fig. S2). A downward drift of CO_2 concentrations would underestimate microbial respiration; however, such effects may be negligible if losses are small relative to microbial respiration rates.

3.2. Soil microbial respiration of rewetted soils: sensor-based method vs. alkali trap method

The sensor platform detected increases in CO_2 concentrations within hours after re-wetting (Fig. 3a). Rates of CO_2 accumulation did not follow a linear pattern during the 4-day incubation. Instead, respiration rates increased rapidly and peaked within 12 hours for most soils, except the forest soils that peaked in respiration approximately 30 hours after re-wetting (Fig 3b). Similar respiration peaks (10–12 hours for cropland soils vs. ~30 hours for forest soils) were observed when soils were incubated using smaller Mason jars (Fig. S3b). Respiration rates calculated using minute rather than four-hour frequency showed similar respiration patterns, although there was much higher variability with the higher temporal resolution (Fig. S4). The temperature inside all soil chambers was maintained at 26 °C during the 4-day incubation, and relative air humidity rapidly increased to near 100% saturation soon after the incubation started (Fig. S5).

Average 4-day microbial respiration increased as soil management intensity decreased, following the order of Till ≤ NoTill ≤ Till_fallow ≤ NoTill_fallow = Hay < Forest (Fig. 3c), and was positively correlated with soil total C content ($r = 0.92$, $p < 0.001$). Average microbial respiration rates calculated from the sensor method were highly correlated with those of the alkali trap method (Fig. 4, $r^2 = 0.89$), and the slope of the linear regression did not deviate from 1. Respiration measurements did not differ between the two methods based on the paired *t*-test comparison ($p = 0.15$).

3.3. Soil water dynamics under drying conditions

The combined use of the digital scale and the CO_2 sensor enabled simultaneous quantification of soil water dynamics and microbial respiration under drying conditions. As expected, the total weight on the digital scale decreased as water evaporated over time (Fig. 5a). Initial net weight of the 5-cm saturated soil columns (22.5 mL) decreased in the order of Till > NoTill > Till_fallow ≥ NoTill_fallow ≥ Hay = Forest (Table1), driven mainly by differences in soil bulk density (Table 1). Cumulative water evaporation was similar among soils in the first three days but was significantly lower in hay soil than other soils after four days (Fig. 5b, Fig. 6). In comparison, relative water evaporation, after accounting for the initial difference in SWC, decreased as management intensity decreased in the order of Till ≥ NoTill = Till_fallow = NoTill_fallow = Hay ≥ Forest (Fig. 5c, Fig. 7). An average of 92% of the initial water in Till soil had evaporated by day 7 while 73% had evaporated in Forest soil (Fig. 7). Differences in evaporation led to differences in SWC during incubation (Fig. 5d, Fig. 8). For instance, volumetric SWC in Hay soil was similar to that of Till soil at day one but was 156% higher than that of Till soil by day 7 (Fig. 8). The observed differences in water evaporation among soils were not caused by variability in incubation conditions because temperature was maintained between 28 °C to 28.5 °C and relative humidity between 15% to 35% throughout the incubation (Fig. S6).

Volumetric SWC at field capacity was similar among cropland soils, which were lower than that in the forest soils before the drying experiment (Table 1). In comparison, volumetric SWC at the end of the drying period increased in the order of Till ≤ NoTill < Till_fallow ≤ NoTill_fallow = Hay < Forest (Fig. 8). Gravimetric SWC followed a similar pattern (Fig. S7). Both volumetric and gravimetric SWC at the end of the drying period were positively correlated

with soil total C content (r = 0.77 and r = 0.92 for volumetric SWC and gravimetric SWC respectively). Water evaporation rates for most soils showed a typical two-stage pattern: evaporation was relatively constant within the first three or four days (stage I) and then rapidly declined afterward (stage II) (Fig. 9). However, evaporation rates for NoTill_fallow and Hay soils continued to decline without an apparent plateau (Fig. 9).

3.5. Comparison of soil microbial respiration under drying conditions vs. consistent soil moisture

Despite SWC declining more than 70% after 7 days, dynamics of microbial respiration under drying conditions were broadly similar to when soils were kept at consistent SWC (Fig. 10 vs. Fig 3b). Microbial respiration at the end of the drying period increased in the order of Till ≤ NoTill ≤ Till_fallow = Hay ≤ NoTill_fallow ≤ Forest (Fig. 10), and showed positive correlations with volumetric SWC (r = 0.53, p = 0.016), gravimetric SWC (r = 0.57, p = 0.010), and soil total C (r = 0.58, p = 0.008).

Direct comparisons of a subset of the soils (i.e., Till_fallow and NoTill_fallow) at the same incubation temperature revealed that cumulative microbial respiration tended to be higher in soils with consistent moisture level as compared to soils incubated under drying conditions (paired t-test, p = 0.07). The lower respiration in drying soils was apparent on day 1 and day 7 (Fig. 11). Respiration was consistently higher in the NoTill_fallow soil than the Till_fallow soil over the 7-day incubation (Fig. 11, Soil management, p < 0.001).

4. Discussion

4.1. Using CO_2 sensors to quantify the temporal dynamics of soil microbial respiration

The ability of the sensor platform to detect differences in CO_2 flux from various land uses and management practices and its congruence with the conventional alkali trap method suggests that inexpensive CO_2 sensors can serve as a promising alternative for quantifying soil microbial respiration. Consistent with our findings, previous studies have showed that similar NDIR CO_2 sensors using a first-order calibration (i.e., calibrated to 400 ppm when exposed to outdoor air) provided accurate measurements of CO_2 gas standards (Djerdj et al., 2021) or comparable readings with other gas analyzers (Joshi Gyawali et al., 2019). CO_2 sensors have been used to detect respiration differences in soils with or without diesel contamination (Kaur et al., 2015) and to quantify microbial responses to different herbicide levels (Djerdj et al., 2021). In addition,

quantifying short-term microbial respiration as a biological indicator of soil health is becoming popular among researchers and other stakeholders working on soil conservation (Wander et al., 2019; Liptzin et al., 2022). The CO_2 sensor platform is portable and does not require hazardous chemicals, making it appealing for use outside of conventional soil analysis labs.

Continuous measurements from CO_2 sensors provided a high temporal resolution in microbial responses to changes in soil water content. Patterns of microbial respiration upon rewetting have been intensively studied and two types of response patterns have been observed (Meisner et al., 2015; Brangarí et al., 2021). The type I response is characterized by respiration being highest immediately (i.e., within minutes) upon rewetting then decreasing gradually (Fraser et al., 2016; Brangarí et al., 2021), and seems to occur when soils were exposed to a short period of drying (i.e., within weeks) (Iovieno and Bååth 2008; Sawada et al., 2016; Slessarev et al., 2020) or when soils only partially dry before rewetting (Meisner et al., 2017). In contrast, the type II response occurs when soils were completely air-dried for a long period of time (i.e., one year or more) before rewetting (Meisner et al., 2013), wherein respiration remains low for an extended period before rapidly increasing with a lag in respiration peaks at ~ 20 hours following rewetting (Meisner et al., 2013, 2015). Consistent with the type II response, soils in our study were air-dried for two years and respiration upon rewetting showed a universal unimodal pattern with respiration peaked at 10-30 hours after rewetting. The mechanism driving the long delay in respiration peaks in our soil, as suggested by Meisner et al. (2013), is likely due to the reduced size of the microbial community that survived the prolonged drying. The resulting high ratio of dissolvable organic C: living microbial biomass after rewetting soils following a prolonged drying period could drive exponential growth for hours coupled with increases in respiration rates. For soils that are air-dried for a short period of time, the population size of surviving microbes remains high, leading to immediately high respiration following rewetting (Type I response). We used the same sensor setup to test soils that were air-dried for two weeks, which showed the same type I respiration pattern as expected (Fig. S8). Our results also revealed a narrow period of time for microbial respiration peaks, suggesting that shape patterns between Type-I and Type-II can be misidentified if discrete measurements fail to capture such "hot moments" in CO_2 flux (Slessarev et al., 2020).

Bursts of respiration upon rapid rewetting of dry soils are well documented in the literature and are often referred to as the "Birch Effect" (Birch and Friend, 1956; Borken and Matzner, 2009). Mechanisms driving this C-flush are not fully understood (see reviews in Schimel, 2018; Barnard et al., 2020), and include microbial metabolism of cytoplasmic solutes that were accumulated to maintain hydration during drying (Fierer and Schimel, 2003; Warren, 2014) as well as microbial utilization of other substrates released from cell lysis upon rewetting (Blazewicz et al., 2020) or previous physically protected SOM (Navarro-García et al., 2012). Respiration peaks observed in our study are consistent with the rapid microbial responses to high availability of labile compounds (either cellular or extracellular) from rewetting. As easily accessible substrates were consumed, microbial respiration rapidly declined. Similar respiration peaks occurred when soils were rewetted to field capacity, suggesting that high CO_2 flux can be dominated by anaerobic respiration, which may promote denitrification processes and trigger pulses of N_2O emission (Leitner et al., 2017). Delayed responses in the Forest soil could be due to its microbial communities being distinct from cropland soils (Gan et al., unpublished data), and it has been shown that different microbial groups resuscitate at different times following rewetting (Placella et al., 2012). Combined with other microbial analyses such as transcriptomics and stable isotope probing analyses (Aanderud et al., 2015), this sensor platform could be a powerful tool in experiments to elucidate temporal dynamics of soil microbial communities and their functional response to dry-wet cycles and other disturbances.

One concern with our incubation system is that increases in CO_2 concentration in the air-tight chambers may suppress microbial respiration (Daniels et al., 1985). MacFadyen (1973) reported that soil respiration measured at a CO_2 concentration of 1700 ppm was 0 to 63% lower than in a CO_2-free atmosphere. Koizumi et al. (1991) found that soil respiration was stimulated when CO_2 concentration was below ambient level, although respiration rates were consistent when CO_2 levels were between 500–1000 ppm. Because the alkali trap method would lower CO_2 concentration below the ambient level, it may over-estimate soil microbial respiration when compared with other closed-chamber or open-flow methods (Bekku et al., 1995). The similarity in microbial respiration obtained between the alkali trap method and the sensor method suggests that the CO_2 concentration effects may be negligible when compared with differences in microbial respiration induced by soil heterogeneity. In addition, respiration rates remain similar when smaller incubation chambers were used (Fig. 3b vs Fig. S3b), suggesting that high CO_2

concentration (up to 10,000 ppm) had little effect on microbial respiration during short-term incubation (i.e., 4–7 days). For longer-term incubation, extremely high cumulated CO_2 concentrations can be avoided by reducing the soil: chamber volume ratio or by including periodic ventilation during incubation.

4.2. Tracking soil water content and water evaporation using digital scales

The evaporation method is a well-established technique to determine soil water retention curves and other soil hydraulic properties in the laboratory (Peters et al., 2015). Similar to data collected by commercial devices such as the HYPROP system (Bezerra-Coelho et al., 2018), water evaporation quantified by the inexpensive sensor platforms exhibited the typical two-stage characteristics: evaporation rate is relatively constant at the beginning (stage I) and then rapidly drops (stage II) when the soil surface becomes dry (Campbell and Norman, 1998). The evaporation rate of the first stage is determined by evaporative demand of the atmosphere (Campbell and Norman, 1998), which was kept consistent across all soil incubations in our study. As a result, the magnitude of stage I evaporation was similar among soils for the first three days (Fig. 6). At the onset of the second drying stage, evaporation rate is determined by the ability of soils to conduct water to the evaporating surface (Lehmann et al., 2008; Han and Zhou, 2013). We believe such empirical evaporation curves generated from the sensor platform can be valuable in modeling soil water evaporation and advancing the theoretical understanding of soil water dynamics in land-surface processes (Bittelli et al., 2008).

Temporal dynamics of SWC is determined by water infiltration and retention following precipitation and water loss to evaporation under drying conditions. SWC at field capacity generally increases as SOM increases (Hudson, 1994), as seen in our study that Forest soil had the highest total C content and the highest SWC at field capacity. In comparison, soil water evaporation is a complex process that is determined by environmental conditions and soil properties such as soil pore size distribution, soil matric potential, soil surface roughness, etc. (Yiotis et al., 2003; Lehmann et al., 2008). Soil structure can be important in affecting water evaporation, and undisturbed soil cores generally have lower evaporation than disturbed soil (Burt et al., 2005). Soils in our study were disturbed (i.e., sieved < 8mm then air dried) before they were loosely packed in soil columns. Hay soils had a lower evaporation and did not have an apparent steady constant rate stage (Fig. 9), which may be partially due to its lower percentage of

water saturation at the beginning (Table 1). However, there is cumulative evidence that mucilage excreted from plant roots and extracellular polysaccharides (EPS) produced by soil bacteria can form biofilms and aggregations that reduce water evaporation and thus conserve more water in soils (Roberson and Firestone, 1992; Kroener et al., 2018; Zheng et al., 2018). Moreover, the addition of EPS in soil has been shown to smoothen the transition between stage-I and stage-II evaporation, reducing the period of the stage I evaporation and total soil water evaporation (Zheng et al. 2018). While more research is needed to confirm the lower evaporation in Hay soils and to investigate links between water evaporation and soil EPS and aggregation levels, we suggest that improving soil resistance to evaporation can be an important strategy to conserve soil water across drying conditions.

4.3. Land use and management effects on soil response to drought

Land use and management practices can profoundly alter soil physicochemical and biological properties, which would further affect a soil's ability to withstand extreme weather events. Consistent with our expectation, volumetric SWC at the end of the drying period increased in the order of Till ≤ NoTill < Till_fallow ≤ NoTill_fallow = Hay < Forest. The ability to retain soil water under drying conditions is essential to maintain soil biological functions, as evidenced from the positive correlation between SWC and microbial respiration at the end of the drying period. Meanwhile, difference in soil C content along the management gradient explained a substantial amount of variation in SWC and microbial respiration, highlighting the central role of SOM in regulating soil water and soil functioning (Rawls et al., 2003; Murphy, 2015). Increase in SOM improves soil water-holding capacity (Lal, 2020) and may also reduce water evaporation by altering aggregation and pore size distribution (Ding et al., 2014). As such, restoring SOM with conservation management practices will be key in improving soil resilience and the development of climate-resilient agriculture (Baveye et al., 2020).

4.4. Caveats and future improvements

The sensor platform consists of inexpensive commercial sensors and electronics and provides continuous and automated measurements of microbial respiration and soil water evaporation during soil incubation. As commercial sensors may come with a wide range of technical specifications, it is important to verify the accuracy, noise levels, and signal drift when using environmental sensors for continuous soil measurements. However, the absolute accuracy

of the sensor readings may not be critical when changes in the measurement values are the point of interest. In addition, the digital scales and CO_2 sensors can be used separately or in combination depending on research interests, and can be configured to integrate other sensors such as soil nitrogen sensors (Fan et al., 2022) to assess soil biological activity for mechanistic evaluations and soil health studies. The simplicity and low cost of the sensor platform has the potential to advance soil resilience research and increase the involvement of stakeholder groups in the development and evaluation of climate-resilient agriculture.

ACKNOWLEDGMENTS

This project is funded by the USDA-NRCS cooperative grant (NR193A750023C018) and the START Proof-of-Concept Fund from the University of Connecticut. We thank NRCS Tolland office for their assistance in soil sampling. We also thank Dr. Beth Lawrence and her graduate student Madeleine Meadows-McDonnell for assisting with the Picarro instrument.

REFERENCES

Aanderud, Z.T., S.E. Jones, N. Fierer, and J.T. Lennon. 2015. Resuscitation of the rare biosphere contributes to pulses of ecosystem activity. Frontiers in Microbiology 6. https://www.frontiersin.org/articles/10.3389/fmicb.2015.00024 (accessed 17 October 2022).

Barnard, R.L., S.J. Blazewicz, and M.K. Firestone. 2020. Rewetting of soil: revisiting the origin of soil CO_2 emissions. Soil Biology and Biochemistry 147: 107819. doi: 10.1016/j.soilbio.2020.107819.

Baveye, P.C., L.S. Schnee, P. Boivin, M. Laba, and R. Radulovich. 2020. Soil organic matter research and climate change: merely re-storing carbon versus restoring soil functions. Frontiers in Environmental Science 8. https://www.frontiersin.org/articles/10.3389/fenvs.2020.579904 (accessed 18 November 2022).

Bekku, Y., H. Koizumi, T. Nakadai, and H. Iwaki. 1995. Measurement of soil respiration using closed chamber method: An IRGA technique. Ecological Research 10(3): 369–373. doi: 10.1007/BF02347863.

Bezerra-Coelho, C.R., L. Zhuang, M.C. Barbosa, M.A. Soto, and M.T. Van Genuchten. 2018. Further tests of the HYPROP evaporation method for estimating the unsaturated soil hydraulic properties. Journal of Hydrology and Hydromechanics 66(2): 161–169. doi: 10.1515/johh-2017-0046.

Birch, H.F., and M.T. Friend. 1956. Humus decomposition in East African soils. Nature 178(4531): 500–501. doi: 10.1038/178500a0.

Bittelli, M., F. Ventura, G.S. Campbell, R.L. Snyder, F. Gallegati, et al. 2008. Coupling of heat, water vapor, and liquid water fluxes to compute evaporation in bare soils. Journal of Hydrology 362(3–4): 191–205. doi: 10.1016/j.jhydrol.2008.08.014.

Blazewicz, S.J., B.A. Hungate, B.J. Koch, E.E. Nuccio, E. Morrissey, et al. 2020. Taxon-specific microbial growth and mortality patterns reveal distinct temporal population responses to rewetting in a California grassland soil. ISME J 14(6): 1520–1532. doi: 10.1038/s41396-020-0617-3.

Borken, W., and E. Matzner. 2009. Reappraisal of drying and wetting effects on C and N mineralization and fluxes in soils. Global Change Biology 15(4): 808–824. doi: 10.1111/j.1365-2486.2008.01681.x.

Brangarí, A.C., S. Manzoni, and J. Rousk. 2021. The mechanisms underpinning microbial resilience to drying and rewetting – A model analysis. Soil Biology and Biochemistry 162: 108400. doi: 10.1016/j.soilbio.2021.108400.

539 Burt, C.M., A.J. Mutziger, R.G. Allen, and T.A. Howell. 2005. Evaporation research: review and
540 interpretation. J. Irrig. Drain Eng. 131(1): 37–58. doi: 10.1061/(ASCE)0733-
541 9437(2005)131:1(37).

542 Campbell, G.S., and J.M. Norman. 1998. Water flow in soil. Introduction to environmental
543 biophysics. 2nd ed. Springer, New York. p. 129–146

544 Dai, A. 2013. Increasing drought under global warming in observations and models. Nature Clim
545 Change 3(1): 52–58. doi: 10.1038/nclimate1633.

546 Daniels, J.A., R. Krishnamurthi, and S.S.H. Rizvi. 1985. A review of effects of carbon dioxide
547 on microbial growth and food quality. Journal of Food Protection 48(6): 532–537. doi:
548 10.4315/0362-028X-48.6.532.

549 Ding, Y., H. Huang, L. Wang, Z.Q. Zhang, and W.H. Zhang. 2014. Effect of different organic
550 matter content on soil moisture dynamics. Applied Mechanics and Materials 477–478:
551 481–484. doi: 10.4028/www.scientific.net/AMM.477-478.481.

552 Djerdj, T., V. Peršić, D. K. Hackenberger, D. K. Hackenberger, and B. K. Hackenberger. 2021.
553 A low-cost versatile system for continuous real-time respiratory activity measurement as
554 a tool in environmental research. Measurement 184: 109928. doi:
555 10.1016/j.measurement.2021.109928.

556 Fan, Y., X. Wang, X. Qian, A. Dixit, B. Herman, et al. 2022. Enhancing the understanding of
557 soil nitrogen fate using a 3D-electrospray sensor roll casted with a thin-layer hydrogel.
558 Environ. Sci. Technol. 56(8): 4905–4914. doi: 10.1021/acs.est.1c05661.

559 Fierer, N., and J.P. Schimel. 2003. A proposed mechanism for the pulse in carbon dioxide
560 production commonly observed following the rapid rewetting of a dry Soil. Soil Science
561 Society of America Journal 67(3): 798–805. doi: 10.2136/sssaj2003.7980.

562 Fox, J., G.G. Friendly, S. Graves, R. Heiberger, G. Monette, et al. 2007. The car package:
563 Companion to applied regression.

564 Franzluebbers, A.J. 2018. Short-term C mineralization (aka the flush of CO2) as an indicator of
565 soil biological health. CAB Reviews. http://doi.org/10.1079/PAVSNNR201813017
566 (accessed 24 May 2022).

567 Franzluebbers, A.J., R.L. Haney, C.W. Honeycutt, H.H. Schomberg, and F.M. Hons. 2000. Flush
568 of Carbon Dioxide Following Rewetting of Dried Soil Relates to Active Organic Pools.
569 Soil Science Society of America Journal 64(2): 613–623. doi:
570 10.2136/sssaj2000.642613x.

571 Fraser, F.C., R. Corstanje, L.K. Deeks, J.A. Harris, M. Pawlett, et al. 2016. On the origin of
572 carbon dioxide released from rewetted soils. Soil Biology and Biochemistry 101: 1–5.
573 doi: 10.1016/j.soilbio.2016.06.032.

574 Gee, G.W., and J.W. Bauder. 1979. Particle size analysis by hydrometer: A simplified method
575 for routine textural analysis and a sensitivity test of measurement parameters 1. Soil
576 Science Society of America Journal 43(5): 1004–1007. doi:
577 10.2136/sssaj1979.03615995004300050038x.

578 van Groenigen, J.W., D. Huygens, P. Boeckx, Th.W. Kuyper, I.M. Lubbers, et al. 2015. The soil
579 N cycle: new insights and key challenges. SOIL 1(1): 235–256. doi: 10.5194/soil-1-235-
580 2015.

581 Han, J., and Z. Zhou. 2013. Dynamics of soil water evaporation during soil drying: laboratory
582 experiment and numerical analysis. The Scientific World Journal 2013: 1–10. doi:
583 10.1155/2013/240280.

584 Hudson, B.D. 1994. Soil organic matter and available water capacity. Journal of Soil and Water
585 Conservation 49(2): 189–194.

586 Iovieno, P., Bååth, E., 2008. Effect of drying and rewetting on bacterial growth rates in soil.
587 FEMS Microbiology Ecology 65, 400–407. doi:10.1111/j.1574-6941.2008.00524.x

588 Joshi Gyawali, A., B.J. Lester, and R.D. Stewart. 2019. Talking SMAAC: a new tool to measure
589 soil respiration and microbial activity. Frontiers in Earth Science 7: 138. doi:
590 10.3389/feart.2019.00138.

591 Kaur, J., V.I. Adamchuk, J.K. Whalen, and A.A. Ismail. 2015. Development of an NDIR CO2
592 sensor-based system for assessing soil toxicity using substrate-induced respiration.
593 sensors 15(3): 4734–4748. doi: 10.3390/s150304734.

594 Koizumi, H., T. Nakadai, Y. Usami, M. Satoh, M. Shiyomi, et al. 1991. Effect of carbon dioxide
595 concentration on microbial respiration in soil. Ecol. Res. 6(3): 227–232. doi:
596 10.1007/BF02347124.

597 Kroener, E., M. Holz, M. Zarebanadkouki, M. Ahmed, and A. Carminati. 2018. Effects of
598 mucilage on rhizosphere hydraulic functions depend on soil particle size. Vadose Zone
599 Journal 17(1): 170056. doi: 10.2136/vzj2017.03.0056.

600 Lal, R. 2020. Soil organic matter and water retention. Agronomy Journal 112(5): 3265–3277.
601 doi: 10.1002/agj2.20282.

602 Lehmann, P., S. Assouline, and D. Or. 2008. Characteristic lengths affecting evaporative drying
603 of porous media. Phys. Rev. E 77(5): 056309. doi: 10.1103/PhysRevE.77.056309.

604 Leitner, S., P.M. Homyak, J.C. Blankinship, J. Eberwein, G.D. Jenerette, et al. 2017. Linking NO
605 and N2O emission pulses with the mobilization of mineral and organic N upon rewetting
606 dry soils. Soil Biology and Biochemistry 115: 461–466. doi:
607 10.1016/j.soilbio.2017.09.005.

608 Lenth, R., and M.R. Lenth. 2018. Package 'lsmeans.' The American Statistician 34(4): 216–221.

609 Liptzin, D., C.E. Norris, S.B. Cappellazzi, G.M. Bean, M. Cope, et al. 2022. An evaluation of
610 carbon indicators of soil health in long-term agricultural experiments. Soil Biology and
611 Biochemistry 172: 108708. doi: 10.1016/j.soilbio.2022.108708.

612 MacFadyen, A. 1973. Inhibitory effects of carbon dioxide on microbial activity in soil.
613 Pedobiologia.

614 Meisner, A., Bååth, E., Rousk, J., 2013. Microbial growth responses upon rewetting soil dried for
615 four days or one year. Soil Biology and Biochemistry 66, 188–192.
616 doi:10.1016/j.soilbio.2013.07.014

617 Meisner, A., A. Leizeaga, J. Rousk, and E. Bååth. 2017. Partial drying accelerates bacterial
618 growth recovery to rewetting. Soil Biology and Biochemistry 112: 269–276. doi:
619 10.1016/j.soilbio.2017.05.016.

620 Meisner, A., J. Rousk, and E. Bååth. 2015. Prolonged drought changes the bacterial growth
621 response to rewetting. Soil Biology and Biochemistry 88: 314–322. doi:
622 10.1016/j.soilbio.2015.06.002.

623 Moyano, F.E., S. Manzoni, and C. Chenu. 2013. Responses of soil heterotrophic respiration to
624 moisture availability: An exploration of processes and models. Soil Biology and
625 Biochemistry 59: 72–85. doi: 10.1016/j.soilbio.2013.01.002.

626 Murphy, B. 2015. Key soil functional properties affected by soil organic matter - evidence from
627 published literature. IOP Conf. Ser.: Earth Environ. Sci. 25(1): 012008. doi:
628 10.1088/1755-1315/25/1/012008.

629 Navarro-García, F., M.Á. Casermeiro, and J.P. Schimel. 2012. When structure means
630 conservation: Effect of aggregate structure in controlling microbial responses to rewetting
631 events. Soil Biology and Biochemistry 44(1): 1–8. doi: 10.1016/j.soilbio.2011.09.019.

632 Norris, C.E., G.M. Bean, S.B. Cappellazzi, M. Cope, K.L.H. Greub, et al. 2020. Introducing the
633 North American project to evaluate soil health measurements. Agronomy Journal 112(4):
634 3195–3215. doi: 10.1002/agj2.20234.Norris

635 Parkin, T.B., Doran, J.W., Franco-Vizcaíno, E., 1997. Field and laboratory tests of soil
636 respiration, in: Methods for Assessing Soil Quality. John Wiley & Sons, Ltd, pp. 231–
637 245. doi:10.2136/sssaspecpub49.c14

638 Peters, A., S.C. Iden, and W. Durner. 2015. Revisiting the simplified evaporation method:
639 Identification of hydraulic functions considering vapor, film and corner flow. Journal of
640 Hydrology 527: 531–542. doi: 10.1016/j.jhydrol.2015.05.020.

641 Placella, S.A., E.L. Brodie, and M.K. Firestone. 2012. Rainfall-induced carbon dioxide pulses
642 result from sequential resuscitation of phylogenetically clustered microbial groups.
643 Proceedings of the National Academy of Sciences 109(27): 10931–10936. doi:
644 10.1073/pnas.1204306109.

R Core Team, R. 2016. R: A language and environment for statistical computing. R Foundation for Statistical Computing, Vienna, Austria.

Rawls, W.J., Y.A. Pachepsky, J.C. Ritchie, T.M. Sobecki, and H. Bloodworth. 2003. Effect of soil organic carbon on soil water retention. Geoderma 116(1): 61–76. doi: 10.1016/S0016-7061(03)00094-6.

Roberson, E.B., and M.K. Firestone. 1992. Relationship between desiccation and exopolysaccharide production in a soil Pseudomonas sp. Applied and Environmental Microbiology 58(4): 1284–1291. doi: 10.1128/aem.58.4.1284-1291.1992.

Schimel, J.P. 2018. Life in dry soils: effects of drought on soil microbial communities and processes. Annu. Rev. Ecol. Evol. Syst. 49(1): 409–432. doi: 10.1146/annurev-ecolsys-110617-062614.

Schindelbeck, R.R., B.N. Moebius-Clune, D.J. Moebius-Clune, K. Kurtz, and H.M. van Es. 2016. Cornell University Comprehensive Assessment of Soil Health Laboratory Standard Operating Procedures.

Seneviratne, S.I., T. Corti, E.L. Davin, M. Hirschi, E.B. Jaeger, et al. 2010. Investigating soil moisture–climate interactions in a changing climate: A review. Earth-Science Reviews 99(3): 125–161. doi: 10.1016/j.earscirev.2010.02.004.

Slessarev, E.W., Y. Lin, B.Y. Jiménez, P.M. Homyak, O.A. Chadwick, et al. 2020. Cellular and extracellular C contributions to respiration after wetting dry soil. Biogeochemistry 147(3): 307–324. doi: 10.1007/s10533-020-00645-y.

Sawada, K., Funakawa, S., Kosaki, T., 2016. Short-term respiration responses to drying–rewetting in soils from different climatic and land use conditions. Applied Soil Ecology 103, 13–21. doi:10.1016/j.apsoil.2016.02.010

Wander, M.M., L.J. Cihacek, M. Coyne, R.A. Drijber, J.M. Grossman, et al. 2019. Developments in agricultural soil quality and health: reflections by the research committee on soil organic matter management. Frontiers in Environmental Science 7. https://www.frontiersin.org/articles/10.3389/fenvs.2019.00109 (accessed 20 November 2022).

Warren, C.R. 2014. Response of osmolytes in soil to drying and rewetting. Soil Biology and Biochemistry 70: 22–32. doi: 10.1016/j.soilbio.2013.12.008.

Wickham, H. 2016. ggplot2: Elegant Graphics for Data Analysis. Springer.

Wood, S.N. 2017. Generalized additive models: an introduction with R. Second edition. CRC Press/Taylor & Francis Group, Boca Raton.

Yiotis, A.G., A.G. Boudouvis, A.K. Stubos, I.N. Tsimpanogiannis, and Y.C. Yortsos. 2003. Effect of liquid films on the isothermal drying of porous media. Phys. Rev. E 68(3): 037303. doi: 10.1103/PhysRevE.68.037303.

681 Zeileis, A., and G. Grothendieck. 2005. zoo: S3 infrastructure for regular and irregular time
682 series. doi: 10.48550/arXiv.math/0505527.

683 Zheng, W., S. Zeng, H. Bais, J.M. LaManna, D.S. Hussey, et al. 2018. Plant growth-promoting
684 rhizobacteria (PGPR) reduce evaporation and increase soil water retention. Water
685 Resources Research 54(5): 3673–3687. doi: 10.1029/2018WR022656.

686 **TABLE**

687 Table 1. Soil physicochemical properties. Values are averages (± SD) from three pedons within each field except for two pedons from
688 the hay field. Different lowercase letters within the same rows indicate statistical differences among soils collected from different land
689 use and management practices according to Tukey's HSD test (p = 0.10).

Soil properties †	Till	NoTill	Till fallow	NoTill fallow	Hay	Forest
Soil Texture	Sandy loam	Sandy loam	Sandy loam	Sandy loam	Sandy loam	Sandy loam
% Clay	8.6 (0.53)	8.2 (0.36)	7.7 (1.19)	10.1 (0.72)	11.3 (1.41)	9.3 (5.81)
% Sand	64.4 (2.25)	60.5 (1.89)	58.2 (4.55)	55.6 (2.12)	57.7 (0.21)	61.4 (12.56)
Total C, mg g^{-1}	23.5 (2.14) a	26.9 (1.1) a	31.3 (2.82) a	52.2 (16.18) b	50.7 (1.95) b	100.6 (7.66) c
Bulk density, g cm^{-3}	1.29 (0.04) d	1.09 (0.03) c	0.99 (0.07) c	0.88 (0.03) b	0.87 (0.04) b	0.7 (0.03) a
Porosity, cm^3 cm^{-3}	0.51 (0.01) a	0.59 (0.01) b	0.63 (0.02) b	0.67 (0.01) c	0.67 (0.02) c	0.74 (0.01) d
SWC at field capacity, cm^3 cm^{-3}	0.41 (0.01) a	0.45 (0.01) a	0.46 (0.03) a	0.46 (0.02) a	0.41 (0.01) a	0.54 (0.05) b
SWC at field capacity, cm^3 g^{-1}	0.32 (0.0004) a	0.41 (0.003) b	0.47 (0.01) c	0.52 (0.03) d	0.47 (0.01) c	0.77 (0.04) e
Saturation level at field capacity, %	0.81 (0.04) b	0.76 (0.03) b	0.74 (0.07) b	0.69 (0.03) ab	0.61 (0.04) a	0.73 (0.08) ab

690 †Soil texture (% sand and % clay) was determined using the hydrometer method (Gee and Bauder, 1979); Total C is measured using a
691 total combustion elemental analyzer (ECS 4010, Costech Analytical Technologies Inc.). Bulk density is calculated based on the net
692 soil weight of the 22.5ml of soil in the loosely packed columns in Experiment II; Porosity is calculated based on bulk density and a
693 mineral density of 2.65 g cm^{-3}. Volumetric and gravimetric SWC (soil water content) at field capacity is described in the method
694 section for Experiment II; Saturation level is calculated based on the volumetric SWC and porosity.

FIGURES LEGENDS

Fig. 1. The novel sensor platform with soil sample, desiccant, environmental sensors, and digital scale inside the air-tight chamber. The micro-controller, display screen and data logger are stationed outside the chamber.

Fig. 2. (a) Relationships between CO_2 concentrations measured by the Piccaro gas analyzer and the CO_2 sensor. (b) Laboratory setup for measuring gas concentration inside the glass jar using the CO_2 sensor and the gas analyzer.

Fig. 3. (a) Cumulative CO_2 concentrations from soil incubations with consistent gravimetric water content (3.75 cm^{-3} g^{-1}). (b) Hourly microbial respiration rates. (c) Averages of microbial respiration rates over 4 days or within each day. Different lowercase letters within the same days indicate statistical differences among soils collected from different land use and management practices according to Tukey's HSD test ($p = 0.10$). Maroon: corn field with conventional till practices; Orange: corn field with no-till practices; Grey: fallow corn field with a history of conventional till practices; Blue: fallow corn field with a history of no-till practices; Green: hay field; Dark green: unmanaged forest.

Fig. 4. Correlation between microbial respiration quantified by the sensor method and the alkali trap method. For both methods, soils were incubated under consistent moisture conditions (3.75 cm^{-3} g^{-1}). Color legend is the same as that in Fig. 3.

Fig. 5. Soil water dynamics when rewetted soils were incubated under drying conditions. (a) Total weight recorded by the digital scales. (b) Cumulative amount of water evaporated. (3). Proportion of cumulative water evaporation. (4) Volumetric soil water content. Color legend is the same as that in Fig. 3.

Fig. 6. Daily averages of cumulative water evaporation when rewetted soils were incubated under drying conditions. Different lowercase letters within the same days indicate statistical differences among soils collected from different land use and management practices according to Tukey's HSD test ($p = 0.10$). Color legend is the same as that in Fig. 3.

Fig. 7. Daily averages of relative water evaporation when rewetted soils were incubated under drying conditions. Different lowercase letters within the same days indicate statistical differences among soils collected from different land use and management practices according to Tukey's HSD test ($p = 0.10$). Color legend is the same as that in Fig. 3.

Fig. 8. Volumetric soil water content when rewetted soils were incubated under drying conditions. Different lowercase letters within the same days indicate statistical differences among soils collected from different land use and management practices according to Tukey's HSD test ($p = 0.10$). Gravimetric soil water content showed a similar pattern in the end of the incubation and was provided in Fig. S5. Color legend is the same as that in Fig. 3.

730 Fig. 9. Hourly water evaporation rates when rewetted soils were incubated under drying
731 conditions. Different lowcase letters indicate statistical differences between days according to
732 Tukey's HSD test (p = 0.10). The shaded areas indicate Stage I evaporation with a relatively
733 steady constant rate. Color legend is the same as that in Fig. 3.

734 Fig. 10. Hourly microbial respiration rates when rewetted soils were incubated under drying
735 conditions. Color legend is the same as that in Fig. 3.

736 Fig. 11. Comparison of soil microbial respiration when incubated under consistent moisture
737 conditions (blue) or drying conditions (orange). Asterisks on day 1 and day 7 indicate significant
738 difference between the two incubation conditions. T/F: Till_Fallow; NT/F: NoTill_Fallow

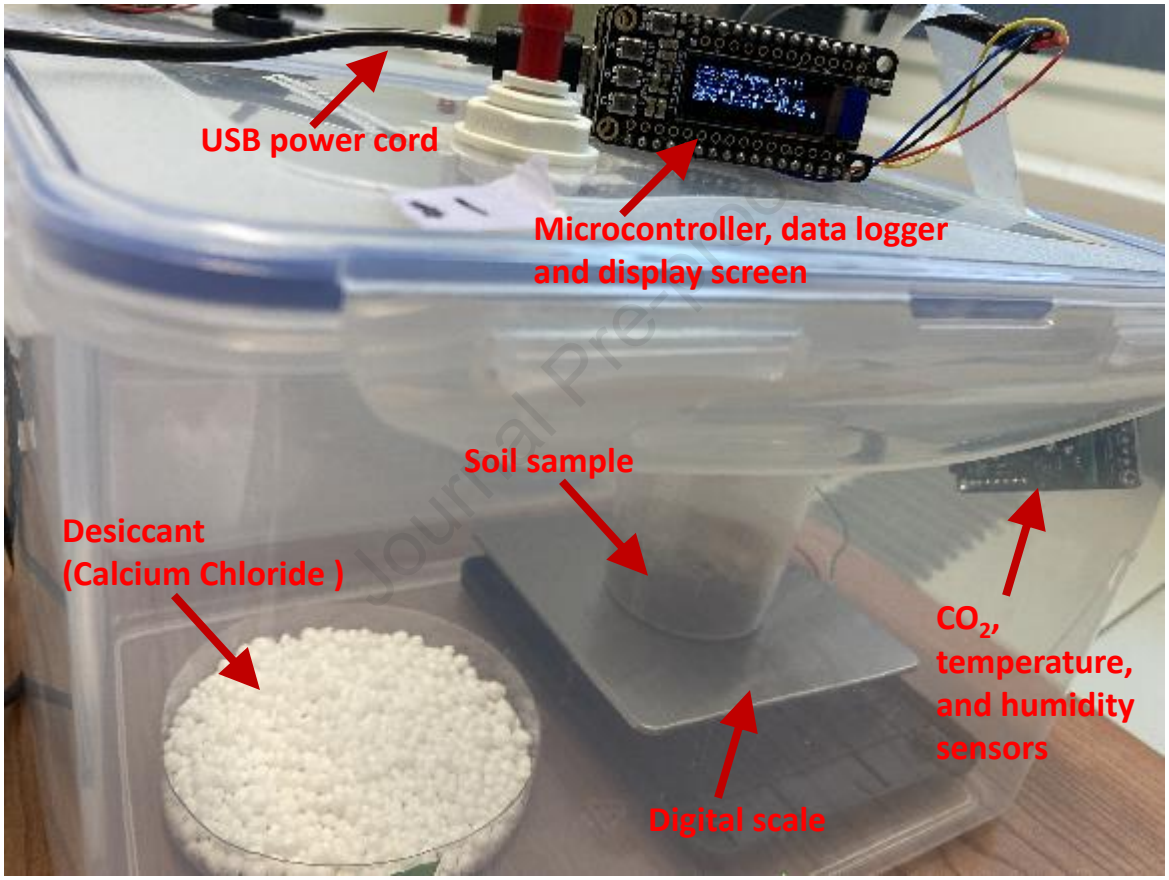
USB power cord
Microcontroller, data logger and display screen
Soil sample
Desiccant (Calcium Chloride)
CO_2, temperature, and humidity sensors
Digital scale

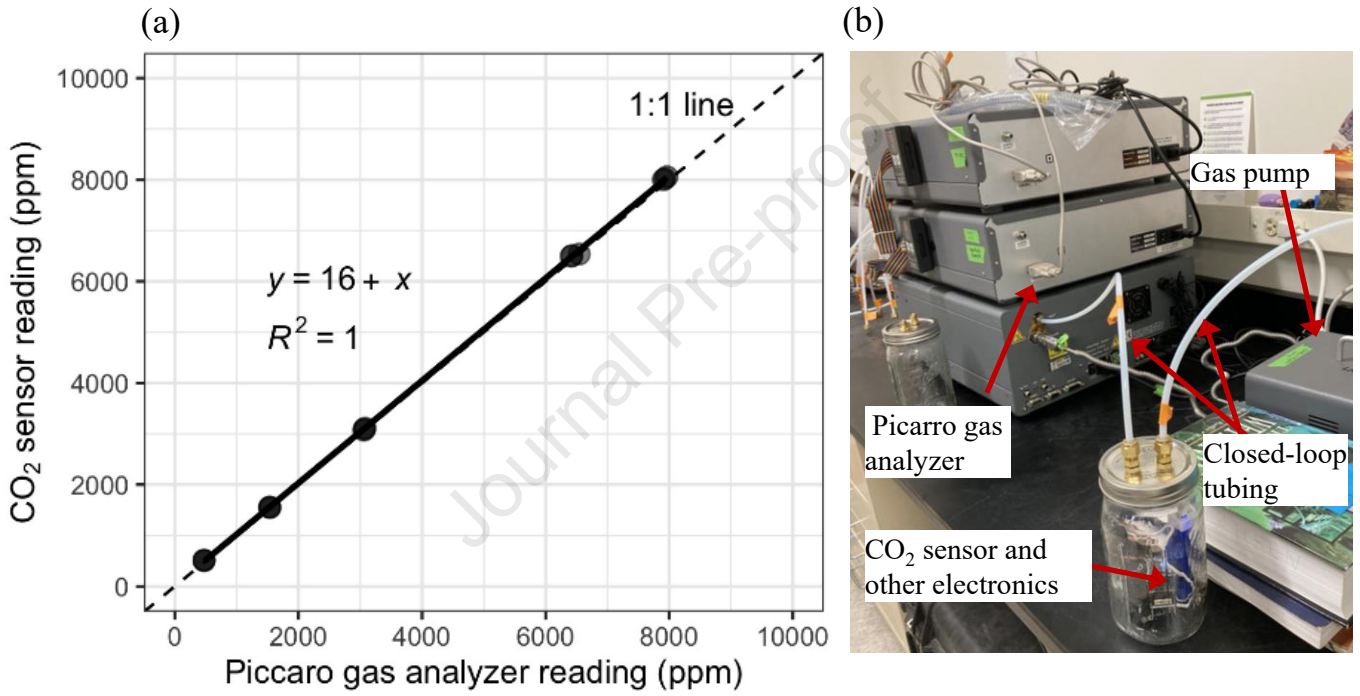

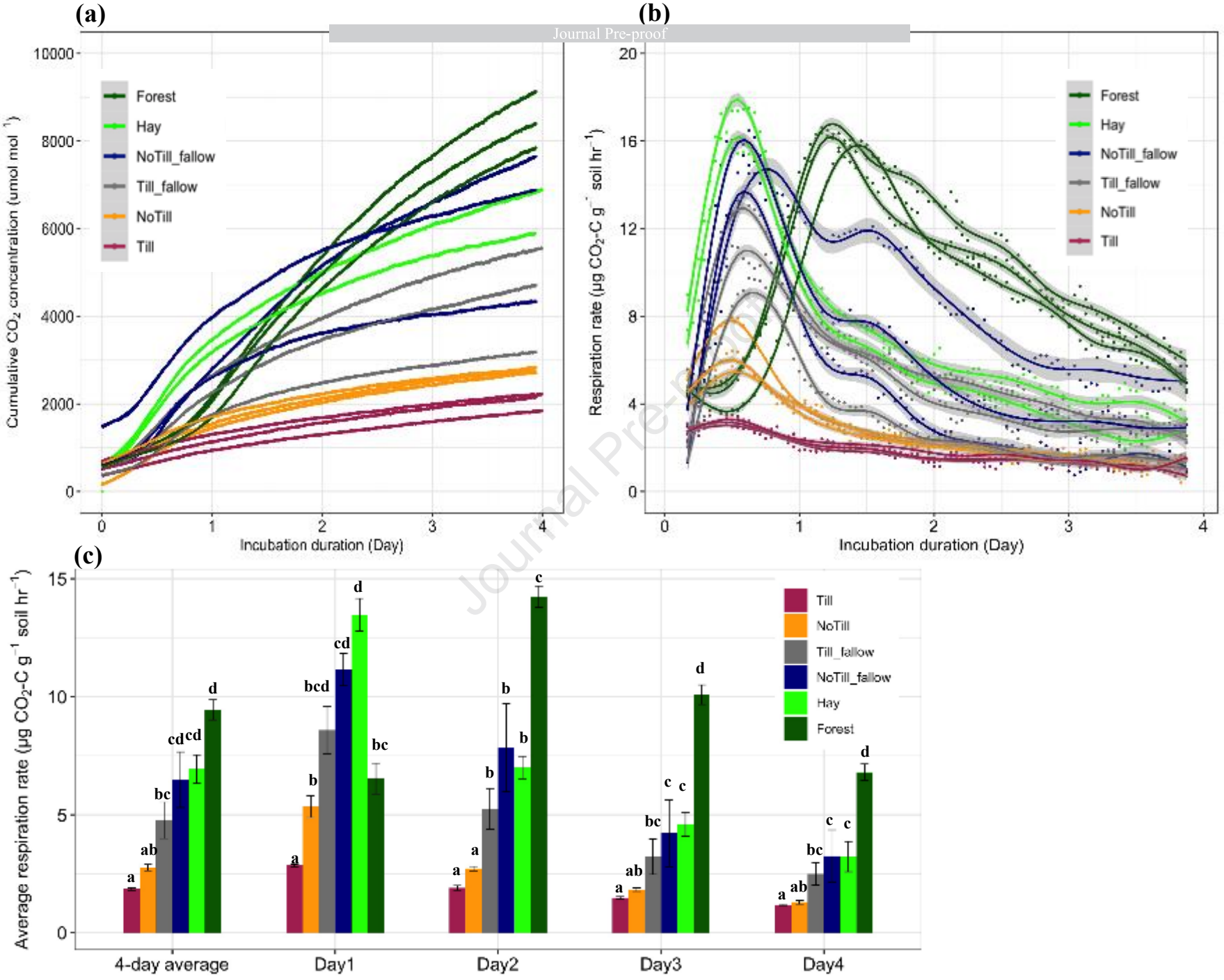

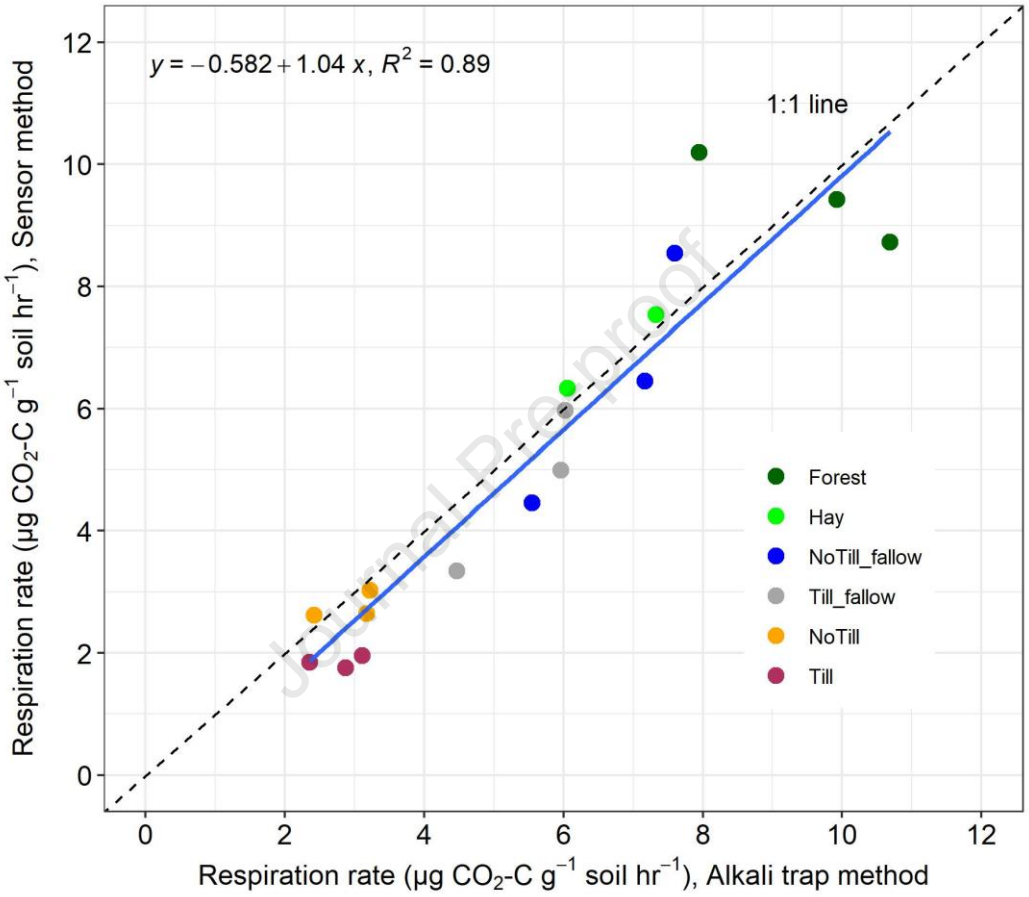

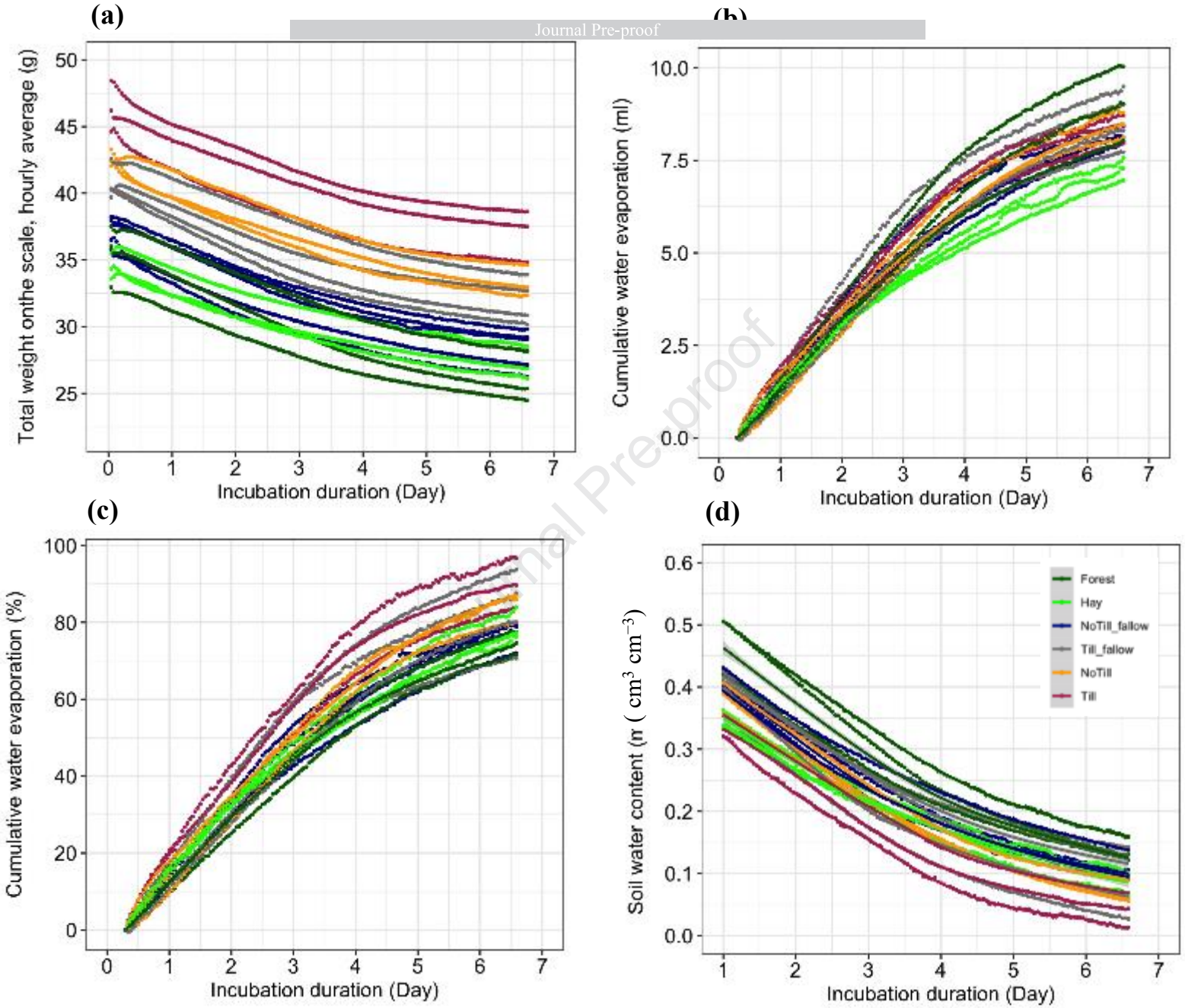

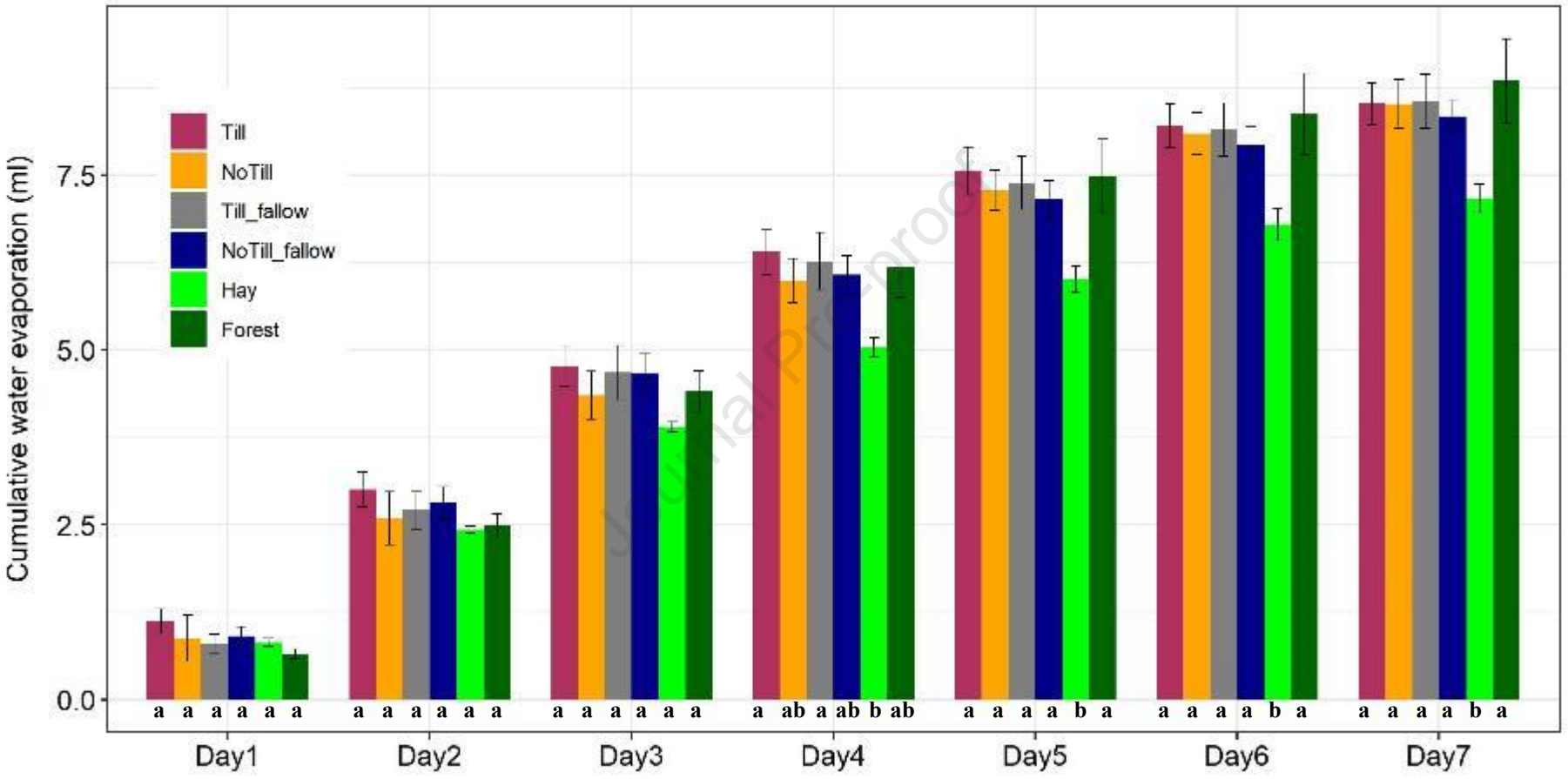

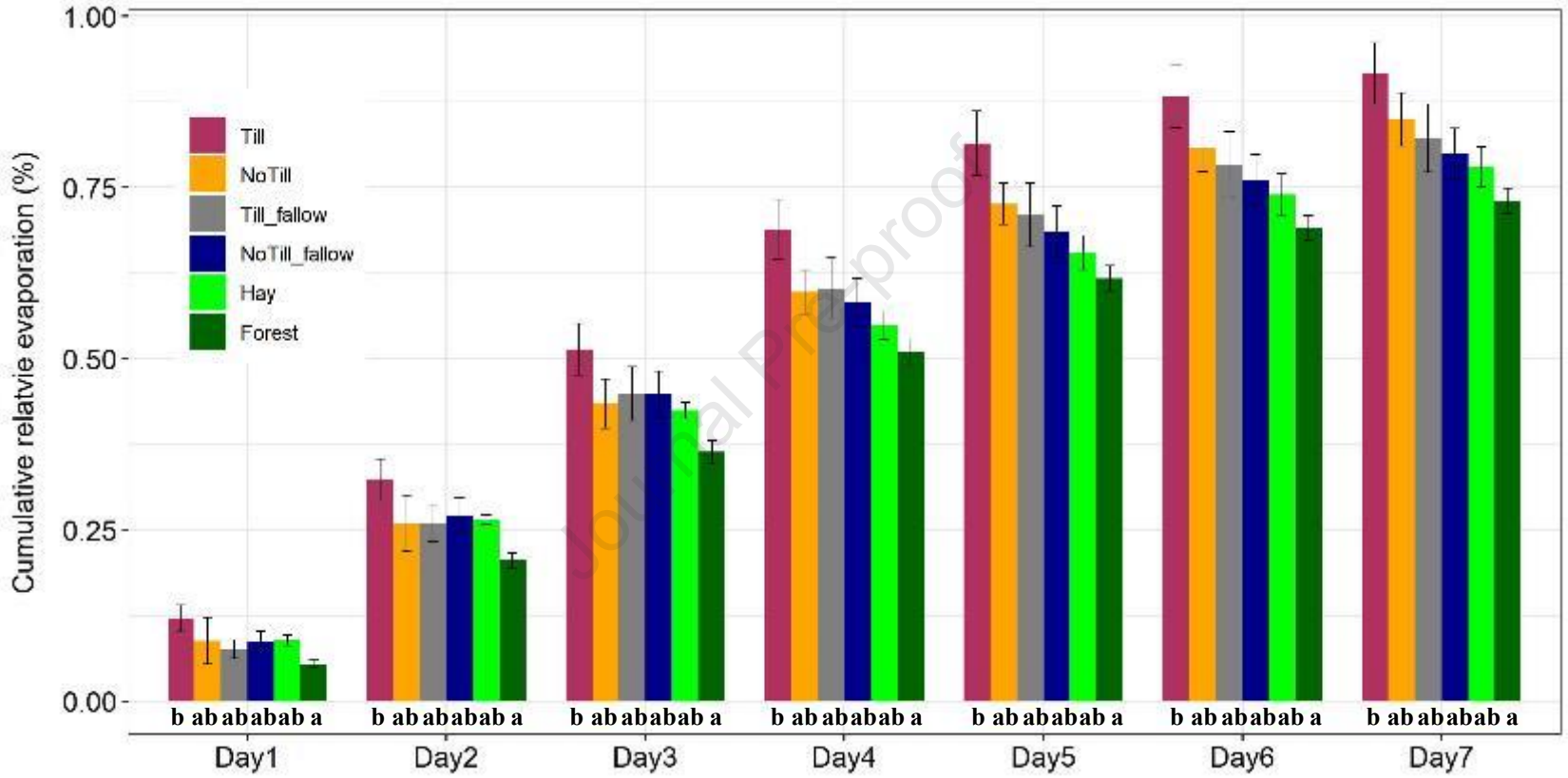

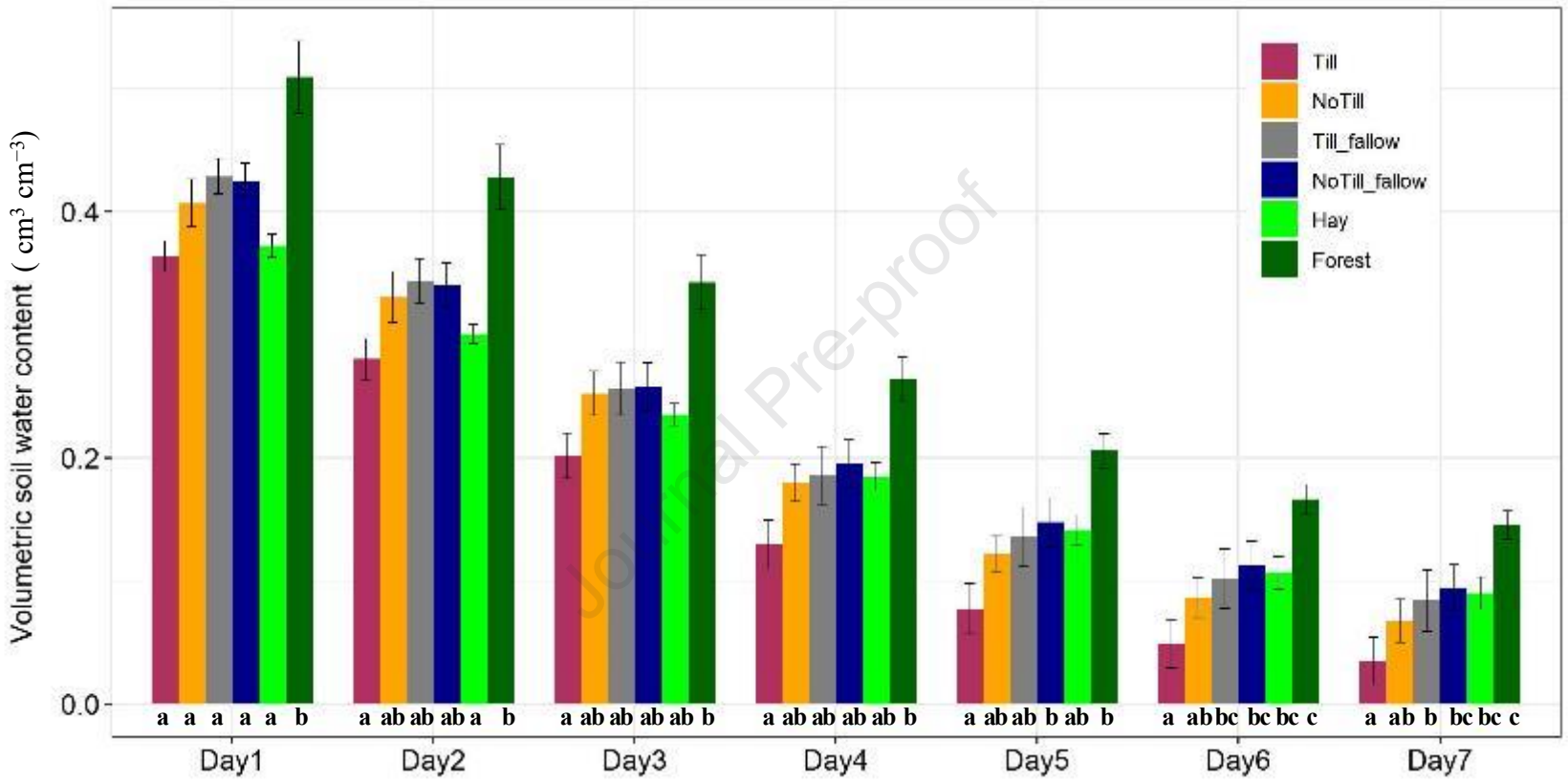

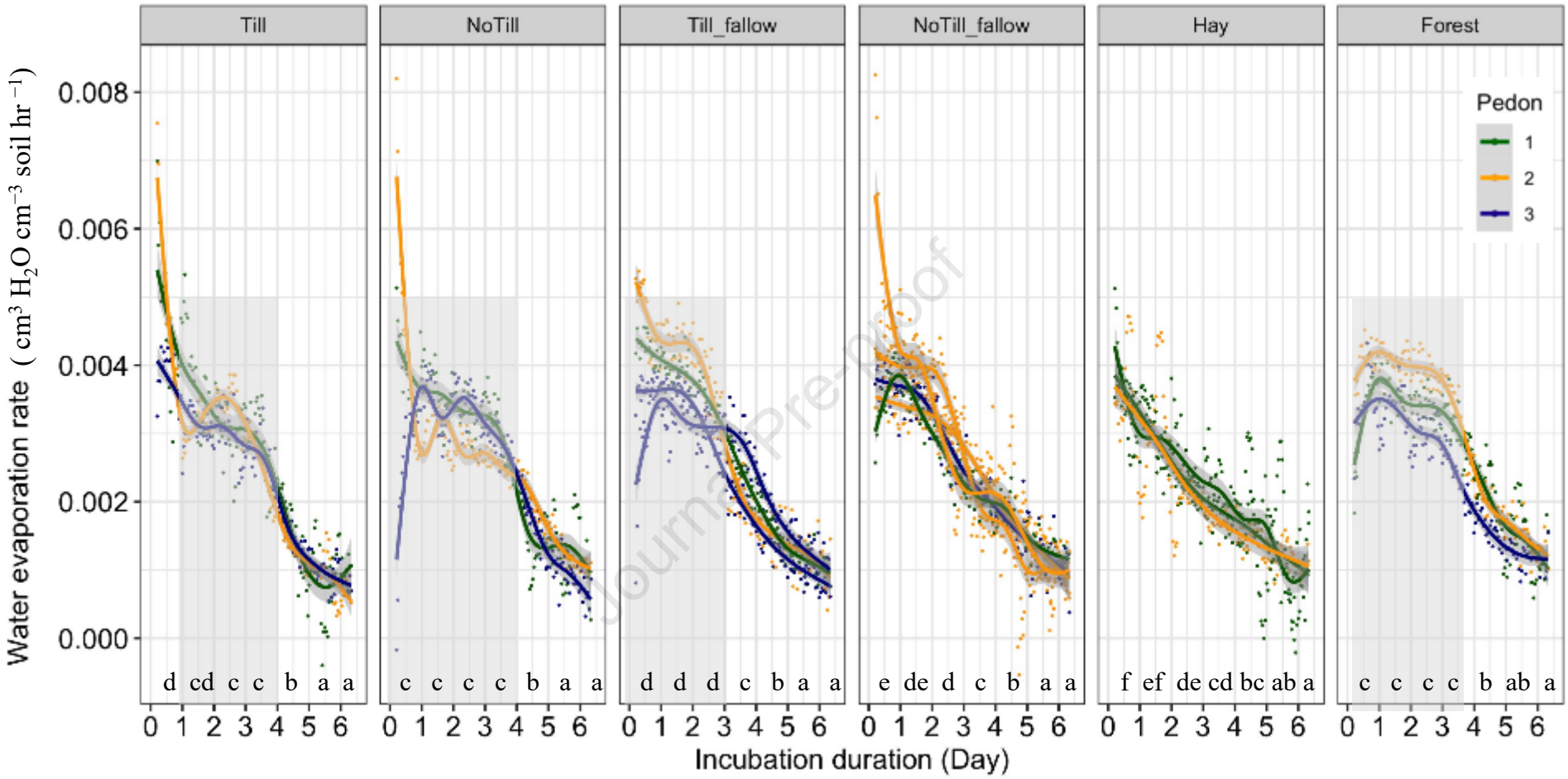

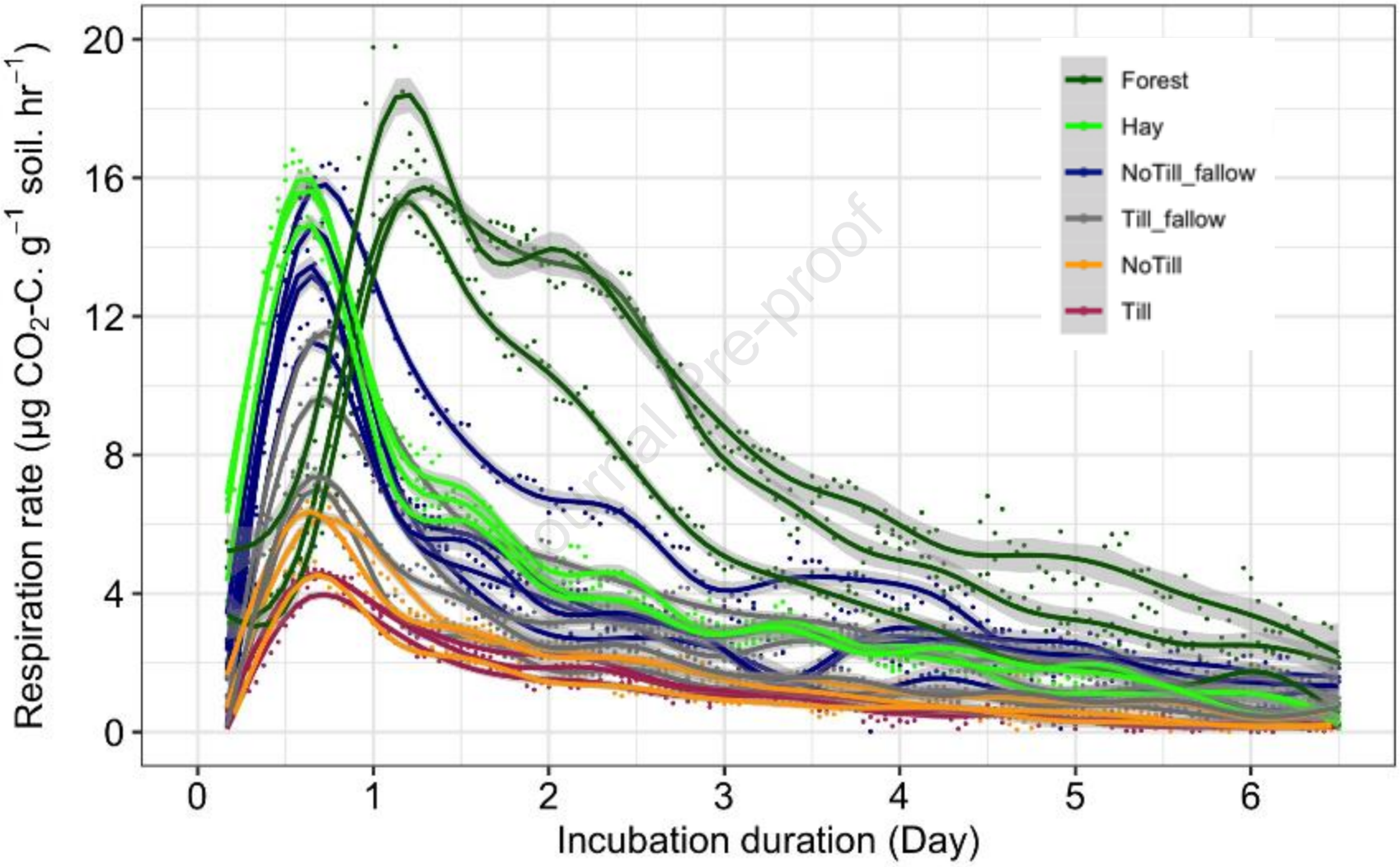

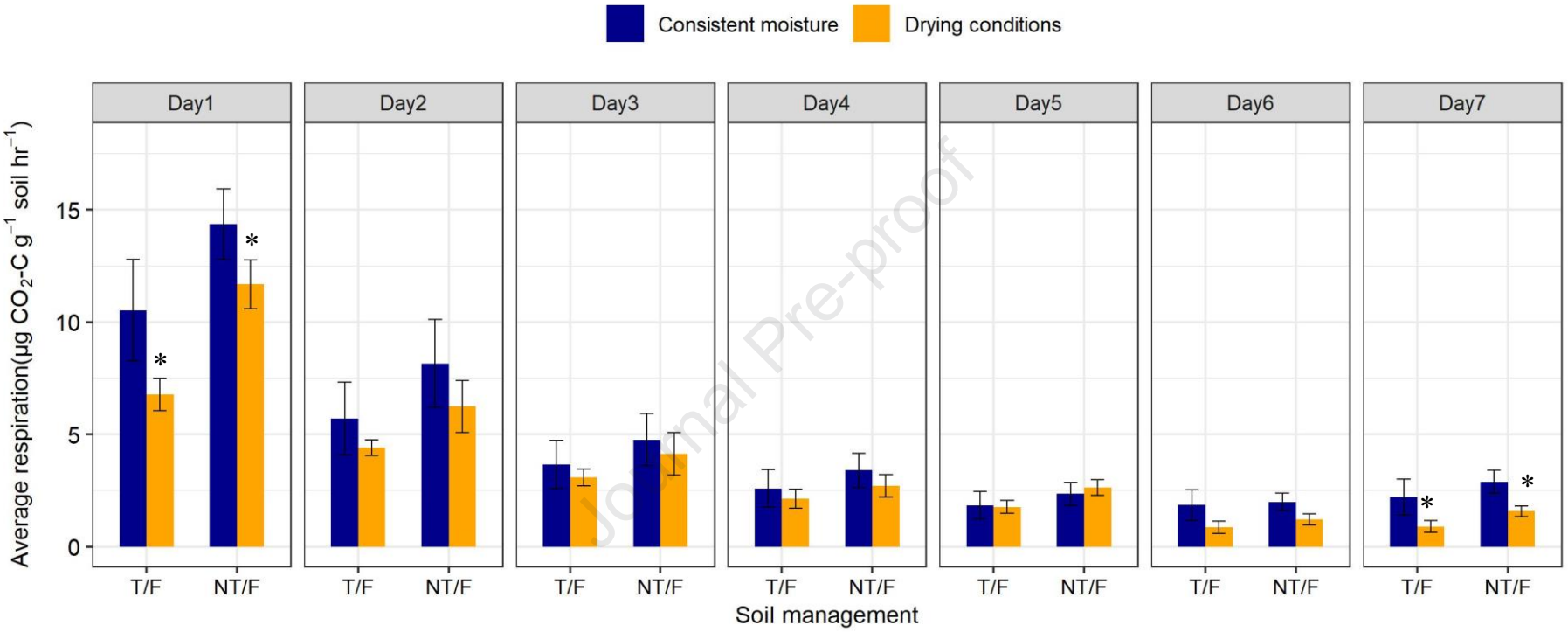

Highlights

- Soil water retention and microbial respiration was quantified using a novel system
- CO_2 sensors provided reliable measurements compared with the alkali trap method
- Respiration was highest in forest soils and declined as management intensified
- Soils with prolonged drying had respiration peaked at 10–30 hr upon rewetting
- Rewetted soil from hay fields had lower evaporation than other soils when drying

Declaration of interests

☒ The authors declare that they have no known competing financial interests or personal relationships that could have appeared to influence the work reported in this paper.

☐ The authors declare the following financial interests/personal relationships which may be considered as potential competing interests: